THE JOURNAL OF PHYSICAL CHEMISTRY B

Article

pubs.acs.org/JPCB

Local Isotropic Diffusion Approximation for Coupled Internal and Overall Molecular Motions in NMR Spin Relaxation

Michelle L. Gill and Arthur G. Palmer, III*

Department of Biochemistry and Molecular Biophysics, Columbia University, 630 West 168th Street, New York, New York 10032, United States

ABSTRACT: The present work demonstrates that NMR spin relaxation rate constants for molecules interconverting between states with different diffusion tensors can be modeled theoretically by combining orientational correlation functions for exchanging spherical molecules with locally isotropic approximations for the diffusion anisotropic tensors. The resulting expressions are validated by comparison with correlation functions obtained by Monte Carlo simulations and are accurate for moderate degrees of diffusion anisotropy typically encountered in investigations of globular proteins. The results are complementary to an elegant, but more complex, formalism that is accurate for all degrees of diffusion anisotropy [Ryabov, Y.; Clore, G. M.; Schwieters, C. D. *J. Chem. Phys.* **2012**, *136*, 034108].

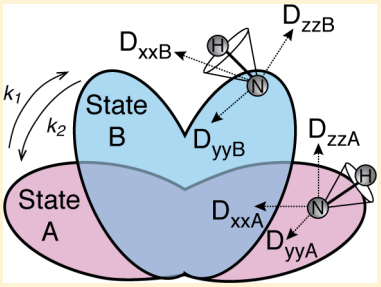

INTRODUCTION

Nuclear magnetic spin relaxation is a consequence of chemical or conformational dynamics of molecules in solution.[1] Over the past 2 decades, ^{2}H, ^{13}C, and ^{15}N spins have been widely employed as probes in NMR spectroscopic studies of proteins and nucleic acids. In well-folded, compact molecules, conformational dynamics on picosecond−nanosecond time scales comparable to or faster than overall rotational diffusion in solution generally have been analyzed assuming a single overall rotational diffusion tensor.[2,3] These techniques, for example, have been applied to ^{15}N spin relaxation of backbone amide groups in hundreds of globular proteins.[4] In the simplest approach, intramolecular motions are regarded as statistically independent or time scale separated from overall motion, leading to the model-free[5,6] or two-step[7] formalisms, respectively. The simplest form of the model-free formalism describes the orientational correlation function as

$$C(\tau) = e^{-\tau/\tau_m}[S^2 + (1 - S^2)e^{-\tau/\tau_e}] \quad (1)$$

in which $\tau_m = 1/(6D_{iso})$ is the rotational correlation time for a spherical molecule with isotropic diffusion constant D_{iso} and S^2 and τ_e are the generalized order parameter and effective internal correlation time, respectively, for internal motions. Extensions to this model include axial or asymmetric diffusion tensors[5−8] and internal motions on two time scales.[9] Approaches in which internal and overall motions are coupled also have been described,[10] but even in these approaches a single well-defined overall rotational diffusion tensor usually is posited[11,12] or additional experimental and computational methods allowing separation of these motions is required.[13,14] These highly successful approaches break down in two limits: (i) unfolded or intrinsically disordered molecules, in which any separation between intramolecular and overall motions is fraught, or (ii) molecular systems whose diffusion tensors are time dependent, owing to conformational changes or folding, oligomerization, or complex formation. A two-domain protein in which the domains are separated by a linker of varying rigidity is a prototypical example in which internal motions that alter the relative orientation of the domains thereby modify the overall rotational diffusion tensor of the molecule. Tjandra and co-workers have used the "extended" two-time-scale model-free formalism to characterize interdomain motions in two-domain proteins, such as calmodulin, while preserving the concept of a single overall diffusion tensor.[15−17]

The complications posed by time-dependent diffusion tensors have been addressed directly by two research groups. Wong and co-workers described a rigorous treatment for the case of interconversion between two or more isotropic diffusion tensors with different diffusion constants and orientations of spin Hamiltonians and extended this approach to axially symmetric tensors under the special condition that the symmetry axes of the tensors are coincident.[18] More recently, Ryabov and co-workers derived an elegant analytical solution for the orientational correlation function for interconverting states with arbitrary diffusion tensors as an expansion in the eigenfunctions of the fully asymmetric diffusion operator.[19] The isotropic system analyzed by Wong and co-workers is analytically tractable, but too restrictive to apply to realistic situations, whereas the results of Ryabov and co-workers are sufficiently complex as to hinder analytical insight.

The main purpose of the present work is to demonstrate that the approach of Wong and co-workers can be extended to more general cases with arbitrary diffusion tensors by incorporating the locally isotropic quadric diffusion approximation of Brüschweiler and co-workers,[20] provided that the relevant diffusion tensors are not highly anisotropic. The results provide a simplified analytically tractable approximation to the general solution of Ryabov and co-workers.

Received: July 2, 2014
Revised: August 27, 2014
Published: August 28, 2014

THEORY

Evolution of the density operator in the interaction frame is described by[21]

$$\frac{d\sigma^{T}(t)}{dt} = -\int_0^\infty d\tau\ \overline{[\mathcal{H}_1^{T}(t), [\mathcal{H}_1^{T}(t-\tau), \sigma^{T}(t) - \sigma_0]]} \tag{2}$$

The stochastic Hamiltonian for an N-site jump process is[22]

$$\mathcal{H}_1(t) = I_z \sum_{j=1}^{N} [f_j(t) - p_j]\omega_{0j} + \sum_{j=1}^{N} f_1(t)\, \mathcal{H}_{1j}(t) \tag{3}$$

in which $f_j(t)$ is unity if the molecule is in conformation j at time t and zero otherwise, $p_j = \langle f_j(t)\rangle$ is the equilibrium population of the jth conformation, ω_{0j} is the Larmor frequency for the spin of interest in the jth conformation, and $\mathcal{H}_{1j}(t)$ is the Hamiltonian for other stochastic processes, such as the fluctuating dipolar interaction, that contribute to relaxation in the jth conformation. Transforming eq 3 into the interaction frame and substituting into eq 2 gives

$$\begin{aligned}\frac{d\sigma^{T}(t)}{dt} &= -[I_z, [I_z, \sigma^{T}(t) - \sigma_0]] \\ &\times \sum_{j,j'} \omega_{0j}\omega_{0j'} \int_0^\infty d\tau\ \overline{[f_j(t) - p_j][f_{j'}(t-\tau) - p_{j'}]} \\ &- \int_0^\infty d\tau \sum_{j,j'} \overline{f_j(t) f_{j'}(t-\tau)[\mathcal{H}_{1j}^{T}(t), [\mathcal{H}_{1j'}^{T}(t-\tau), \sigma^{T}(t) - \sigma_0]]}\end{aligned} \tag{4}$$

The first term on the right-hand side of this equation represents relaxation due to chemical exchange broadening; this classical relaxation mechanism has been treated in this formalism by Abergel and Palmer[22] and is not treated further herein. However, this term makes evident that application of the Redfield formalism in the present case requires that the N-site jump processes are fast on the chemical shift time scale; this implies that only a single population-averaged resonance line is observed in the NMR spectrum. However, the jump process may be slow (or fast) on the time scale of the stochastic Hamiltonians $\mathcal{H}_{1j}(t)$, which typically will vary on the rotational diffusion time scale. If this time-scale restriction is not satisfied, then the full stochastic Liouville approach becomes necessary.[22]

If the N-site jump processes are time-scale separated from the stochastic processes $\mathcal{H}_{1j}(t)$, then

$$\begin{aligned}\frac{d\sigma^{T}(t)}{dt} &= -[I_z, [I_z, \sigma^{T}(t) - \sigma_0]] \\ &\times \sum_{j,j'} \omega_{0j}\omega_{0j'} \int_0^\infty d\tau\ \overline{[f_j(t) - p_j][f_{j'}(t-\tau) - p_{j'}]} \\ &- \int_0^\infty d\tau \sum_{j,j'} \langle f_j(t) f_{j'}(t-\tau)\rangle \overline{[\mathcal{H}_{1j}^{T}(t), [\mathcal{H}_{1j'}^{T}(t-\tau), \sigma^{T}(t) - \sigma_0]]}\end{aligned} \tag{5}$$

in which the stochastic correlation function for the jump process is $\langle f_j(t)\, f_{j'}(t-\tau)\rangle$. If the jump processes are fast compared to the other stochastic processes, then the long-time value is reached on a time scale that is short compared to the stochastic processes, $\mathcal{H}_{1j}(t)$:

$$\langle f_j(t) f_{j'}(t-\tau)\rangle \to p_j p_{j'} \tag{6}$$

Making this substitution recovers the general fast-limit result:

$$\begin{aligned}\frac{d\sigma^{T}(t)}{dt} &= -[I_z, [I_z, \sigma^{T}(t) - \sigma_0]] \\ &\times \sum_{j,j'} \omega_{0j}\omega_{0j'} \int_0^\infty d\tau\ \overline{[f_j(t) - p_j][f_{j'}(t-\tau) - p_{j'}]} \\ &- \int_0^\infty d\tau\ \overline{[\langle \mathcal{H}_1(t)\rangle^{T}, [\langle \mathcal{H}_1(t-\tau)\rangle^{T}, \sigma^{T}(t) - \sigma_0]]}\end{aligned} \tag{7}$$

in which

$$\langle \mathcal{H}_1(t)\rangle = \sum_{j=1}^{N} p_j \mathcal{H}_{1j}(t) \tag{8}$$

is the population-average stochastic Hamiltonian. If the jump process is slow compared to the other stochastic processes, then

$$\langle f_j(t) f_{j'}(r-\tau)\rangle \to p_j p_{jj'} \tag{9}$$

Making this substitution recovers the general slow-limit result:

$$\begin{aligned}\frac{d\sigma^{T}(t)}{dt} &= -[I_z, [I_z, \sigma^{T}(t) - \sigma_0]] \\ &\times \sum_{j,j'} \omega_{0j}\omega_{0j'} \int_0^\infty d\tau\ \overline{[f_j(t) - p_j][f_{j'}(t-\tau) - p_{j'}]} \\ &- \sum_{j=1}^{N} p_j \int_0^\infty d\tau\ \overline{[\mathcal{H}_{1j}^{T}(t), [\mathcal{H}_{1j}^{T}(t-\tau), \sigma^{T}(t) - \sigma_0]]}\end{aligned} \tag{10}$$

In the fast limit, the stochastic Hamiltonian is averaged, and the resulting relaxation rate constant is determined by the stochastic fluctuations of the averaged Hamiltonian. In the slow limit, the correlation functions (equivalently, the spectral density functions or relaxation rate constants) are averaged. In the above limits, no additional assumptions need to be made about the stochastic processes; that is, rotational diffusion can be quite general and internal motions can be present.

Between these two limits, the analysis proceeds as usual by expanding the stochastic Hamiltonians in irreducible tensor operators:[21]

$$\mathcal{H}_1(t) = \sum_{q=-2}^{2} \sum_{p} (-1)^q F_2^{-q}(t) \mathbf{A}_{2p}^{q} \tag{11}$$

which yields upon substitution into eq 4

$$\begin{aligned}\frac{d\sigma^{T}(t)}{dt} &= -[I_z, [I_z, \sigma^{T}(t) - \sigma_0]] \\ &\times \sum_{j,j'} \omega_{0j}\omega_{0j'} \int_0^\infty d\tau\ \overline{[f_j(t) - p_j][f_{j'}(t-\tau) - p_{j'}]} \\ &- \sum_{q=-2}^{2} \sum_{p} [\mathbf{A}_{2p}^{-q}, [\mathbf{A}_{2p}^{-q}, \sigma^{T}(t) - \sigma_0]] \\ &\times \int_0^\infty \exp\{-i\omega_p^q \tau\}\, d\tau \sum_{j,j'} \overline{f_j(t) f_{j'}(t-\tau) F_{2j}^{-q}(t) F_{2j'}^{-q}(t-\tau)}\end{aligned} \tag{12}$$

In the simplest case, $F_{2j}^{q}(t) = c_j Y_2^{q}[\Omega_j(t)]$, in which c_j is a (assumed constant) function of physical parameters associated with the stochastic Hamiltonian, and the correlation function

$$\begin{aligned}&\overline{f_\alpha(t) f_{j'}(t-\tau)\, F_{2j'}^{q}(t)\, F_{2j'}^{-q}(t-\tau)} \\ &= c_j c_{j'} \langle f_j(0) f_{j'}(\tau)\, Y_2^{q}[\Omega_j(0)]\, Y_2^{-q}[\Omega_{j'}(\tau)]\rangle \\ &= c_j c_{j'} C_{jj'}^{q}(\tau)\end{aligned} \tag{13}$$

dx.doi.org/10.1021/jp506580c | J. Phys. Chem. B 2014, 118, 11120−11128

is calculated by using

$$C^q_{jj'}(\tau) = \int\int d\Omega\, d\Omega'\, Y^q_2(\Omega)\, Y^{-q}_2(\Omega')\, p_{jj'}(\Omega', \tau; \Omega, 0)\, p_j(\Omega, 0) \tag{14}$$

in which $p_j(\Omega,0)$ is the probability that the molecule is in conformation j with orientation Ω at time 0 and $p_{jj'}(\Omega',\tau;\Omega,0)$ is the conditional probability that the molecule is in conformation j', with orientation Ω' at time τ; given that it was in conformation j with orientation Ω at time 0. In isotropic solution $C^q_{jj'}(\tau) = (-1)^q C_{jj'}(\tau)$, therefore, only the correlation function $C^0_{jj'}(\tau) = C_{jj'}(\tau)$ needs to be calculated:

$$C_{jj'}(\tau) = \int\int d\Omega\, d\Omega'\, Y^0_2(\Omega)\, Y^0_2(\Omega')\, p_{jj'}(\Omega', \tau; \Omega, 0)\, p_j(\Omega, 0) \tag{15}$$

Methods for calculating this correlation function have been presented by Wong and co-workers[18] and Ryabov and co-workers.[19]

In the simplest illustrative case, previously analyzed by Wong and co-workers,[18] the molecule undergoes jumps between N rigid conformations with isotropic diffusion tensors D_j. The stochastic Hamiltonians also are assumed to have axial symmetry, and the orientations of the unique axes are defined by unit vectors $\boldsymbol{\mu}_j$, for $j = 1, N$. In the case of dipole−dipole relaxation between two covalently bonded atoms, the unit vectors are oriented along the bond. Using the transformation properties of the irreducible spherical tensors:

$$Y^0_2(\Omega') = \sum_{k=-2}^{2} D^2_{k0}[\Omega^{BF}]\, Y^k_2(\Omega_{j'}) \tag{16}$$

in which Ω^{BF} are the Euler angles defining the transformation from an internal body frame (superimposed on the frame of conformation j) to the laboratory reference frame for the conformation j' and $\Omega_{jj'}$ are the spherical coordinates of $\mu_{j'}$ in the internal frame (without loss of generality this frame can be oriented with its z-axis parallel to $\boldsymbol{\mu}_j$). Noting that $p_{jj'}(\Omega,0;\Omega_0,0) = \delta_{jj'}\delta(\Omega - \Omega_0)$ yields $p_{jj'}(\Omega,t;\Omega_0,0) = \delta(\Omega - \Omega_0)a_{jj'}(\Omega,t;\Omega_0,0)$ and the conditional probabilities are determined from[18]

$$\frac{da_{jj'}(\Omega, t; \Omega_0, 0)}{dt} = j\sum_{\gamma=1}^{N} k_{j\gamma}a_{\gamma j'}(\Omega, t; \Omega_0, 0) - 6\tilde{D}_j a_{jj'}(\Omega, t; \Omega_0, 0) \tag{17}$$

in which $k_{jj'}$ is the rate constant for transitions from state j to j', $k_{jj} = -\Sigma_{j\neq j'} K_{jj'}$ and $a_{jj'}(\Omega,0;\Omega_0,0) = \delta_{jj'}$. Substituting these results into eq 15 and performing the integrals gives

$$C_{jj'}(\tau) = Y^0_2(\boldsymbol{\mu}_j\cdot\boldsymbol{\mu}_{j'})\, a_{jj'}(\Omega^{BF}, \tau; \Omega, 0)\, p_j(\Omega, 0) \tag{18}$$

This result, together with the identity $C^q_{jj'}(\tau) = (-1)^q C_{jj'}(\tau)$, is substituted into eq 13 to complete the derivation of the correlation function needed in the expression for the time dependence of the density operator, eq 12.

For $N = 2$ states, denoted A and B, with diffusion constants D_A and D_B, interaction vectors $\boldsymbol{\mu}_A$ and $\boldsymbol{\mu}_B$, and assuming $c_A = c_B$, Wong and co-workers showed that the orientational correlation function has the form of the model-free correlation function:[18]

$$C(\tau) = \sum_{j,j'} C_{jj'}(\tau) = e^{-6D\tau}[S^2 + (1 - S^2)e^{-k\tau}] \tag{19}$$

in which

$$k = [k^2_{ex} + 12(D_A - D_B)(k_1 - k_2) + 36(D_A - D_B)^2]^{1/2}$$
$$S^2 = \frac{1}{2}\left[1 + \frac{(k_1 - k_2)(6D_A - 6D_B + k_1 - k_2) + 4k_1k_2Y^0_2(\boldsymbol{\mu}_A\cdot\boldsymbol{\mu}_B)}{kk_{ex}}\right]$$
$$6D = 3(D_A + D_B) + (k_{ex} - k)/2 \tag{20}$$

$k_{ex} = k_1 + k_2$, k_1 and k_2 are the rate constants for transitions from state A to B, and from state B to A, respectively.

When $k_{ex} \gg (D_A - D_B)$,

$$k \approx k_{ex} - 6(D_A - D_B)(p_A - p_B) \approx k_{ex}$$
$$S^2 \approx 1 - 2p_Ap_B[1 - Y^0_2(\boldsymbol{\mu}_j\cdot\boldsymbol{\mu}_{j'})] = 1 - 3p_Ap_B\sin^2(\boldsymbol{\mu}_A\cdot\boldsymbol{\mu}_B)$$
$$6D \approx 6(p_AD_A + p_BD_B) = 6\bar{D} \tag{21}$$

in which the expression for S^2 is the usual generalized order parameter for a two-site jump process, $\bar{D}$ is the population-average diffusion constant, and $p_A = k_2/k_{ex}$ and $p_B = k_1/k_{ex}$ are the equilibrium populations of the two states. The correlation function becomes

$$C(\tau) = S^2e^{-6\bar{D}\tau} = [1 - 3p_Ap_B\sin^2(\boldsymbol{\mu}_A\cdot\boldsymbol{\mu}_B)]e^{-6\bar{D}\tau} \tag{22}$$

Consistent with the earlier fast-limit result, eq 22 is the correlation function for the population average of the two stochastic Hamiltonians. This limit is essentially equivalent to the extended model-free formalism used by Tjandra and co-workers to characterize interdomain motion,[15] except that the scalar product between $\boldsymbol{\mu}_A$ and $\boldsymbol{\mu}_B$ incorporates both reorientation of the domains and reorientation of the equilibrium orientations of the interaction vectors within the two domains.

When $k_{ex} \ll (D_A - D_B)$,

$$k \approx 6(D_A - D_B) + k_1 - k_2 \approx 6(D_A - D_B)$$
$$S^2 = p_B$$
$$6D = 6D_B \tag{23}$$

The correlation function becomes

$$C(\tau) = p_Ae^{-6D_A\tau} + p_Be^{-6D_B\tau} \tag{24}$$

Consistent with the earlier slow-limit result, eq 24 is the population average of the individual correlation functions for the two stochastic Hamiltonians. Because nuclear spin relaxation rate constants depend linearly on the spectral density function, which in turn is the Fourier transform of $C(\tau)$, the relaxation rate constants themselves become the population-weighted averages of the rate constants for each state.

As noted by Wong and co-workers, more general cases in which the diffusion tensors of the interconverting conformations are not isotropic are much more complex.[18] However, in many cases of interest, the degree of anisotropy of the diffusion tensor is relatively modest. In these cases, Brüschweiler and co-workers have shown that anisotropic rotational diffusion can be treated with an effective locally isotropic diffusion tensor given by[20]

$$\tilde{D} = \mathbf{e}^T\mathbf{Q}\mathbf{e} \tag{25}$$

in which $\mathbf{e}$ are the directions cosines defining the orientation of $\boldsymbol{\mu}$ in the principal frame of the diffusion tensor, $\mathbf{Q}$ is diagonal

dx.doi.org/10.1021/jp506580c | J. Phys. Chem. B 2014, 118, 11120−11128

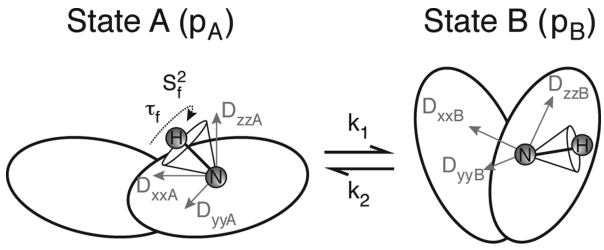

Figure 1. Schematic of dynamic parameters for an enzyme undergoing conformational exchange. The two conformations, denoted "A" and "B", have equilibrium populations p_A and p_B, respectively. A representative amide bond is depicted in both conformations. The effective internal correlation time is τ_f and the square of the generalized order parameter is S_f^2 for fast intramolecular motions of the amide bond. The amide bond is shown superimposed on the enzyme diffusion axes (gray), denoted D_{xxj}, D_{yyj}, and D_{zzj}, where j indicates either state A or B. The rate constant for transitions from open to closed conformations is k_1, while the reverse rate constant is k_2.

with elements $Q_{xx} = (D_{yy} + D_{zz})/2$, $Q_{yy} = (D_{xx} + D_{zz})/2$, and $Q_{zz} = (D_{xx} + D_{yy})/2$, and D_{ii} are the principal values of the diffusion tensor. For an axially symmetric diffusion tensor, $D_{xx} = D_{yy} = D_\perp$ and $D_{zz} = D_\parallel$, and errors in $D_\parallel/D_\perp$ and $(D_\parallel + 2D_\perp)/3$ obtained from this approximation are less than 10% for $0.65 \leq D_\parallel/D_\perp \leq 1.75$.[23]

When the approximation of eq 25 applies, the general situation can be treated as jumps among N conformations with N local isotropic diffusion constants $\tilde{D}_j$ and $N(N-1)/2$ intervector angles, given by $\boldsymbol{\mu}_j \cdot \boldsymbol{\mu}_{j'}$, between axially symmetric stochastic Hamiltonians using eqs 17 and 18. For two-site ($N = 2$) exchange, the results are given by eqs 19 and 20, with D_A and D_B replaced by $\tilde{D}_A$ and $\tilde{D}_B$, respectively. This simplification of the general problem, depicted in Figure 1, to an approximately isotropic one is a main result of this work.

For completeness, although not utilized herein, fast internal motions that are statistically independent of overall diffusional and jump motions, such as librations of a given bond vector, can be incorporated into the correlation function by defining a total correlation function:[5,6]

$$G(t) = C(t)\{S_f^2 + (1 - S_f^2)e^{-t/\tau_f}\} \tag{26}$$

in which S_f^2 and τ_f are the square of the generalized order parameter and effective internal correlation time for the fast intramolecular motion, respectively.

Recently, considerable interest has arisen in detecting conformational changes in proteins and RNA molecules on time scales longer than rotational diffusion and shorter than the time scale for chemical exchange broadening.[24,25] This time scale is the preceding slow-limit result, in which the relaxation rate constants (or spectral density or correlation functions) are averaged. For heteronuclear spin relaxation of H–X spin pairs (X = ^{15}N or ^{13}C),

$$(R_2 - 0.5R_1)/R_1 \approx \frac{2}{3}\langle\tilde{\tau}_{mj}\rangle\left\langle\frac{\tilde{\tau}_{mj}}{1 + \tilde{\tau}_{mj}^2\omega_X^2}\right\rangle^{-1} \tag{27}$$

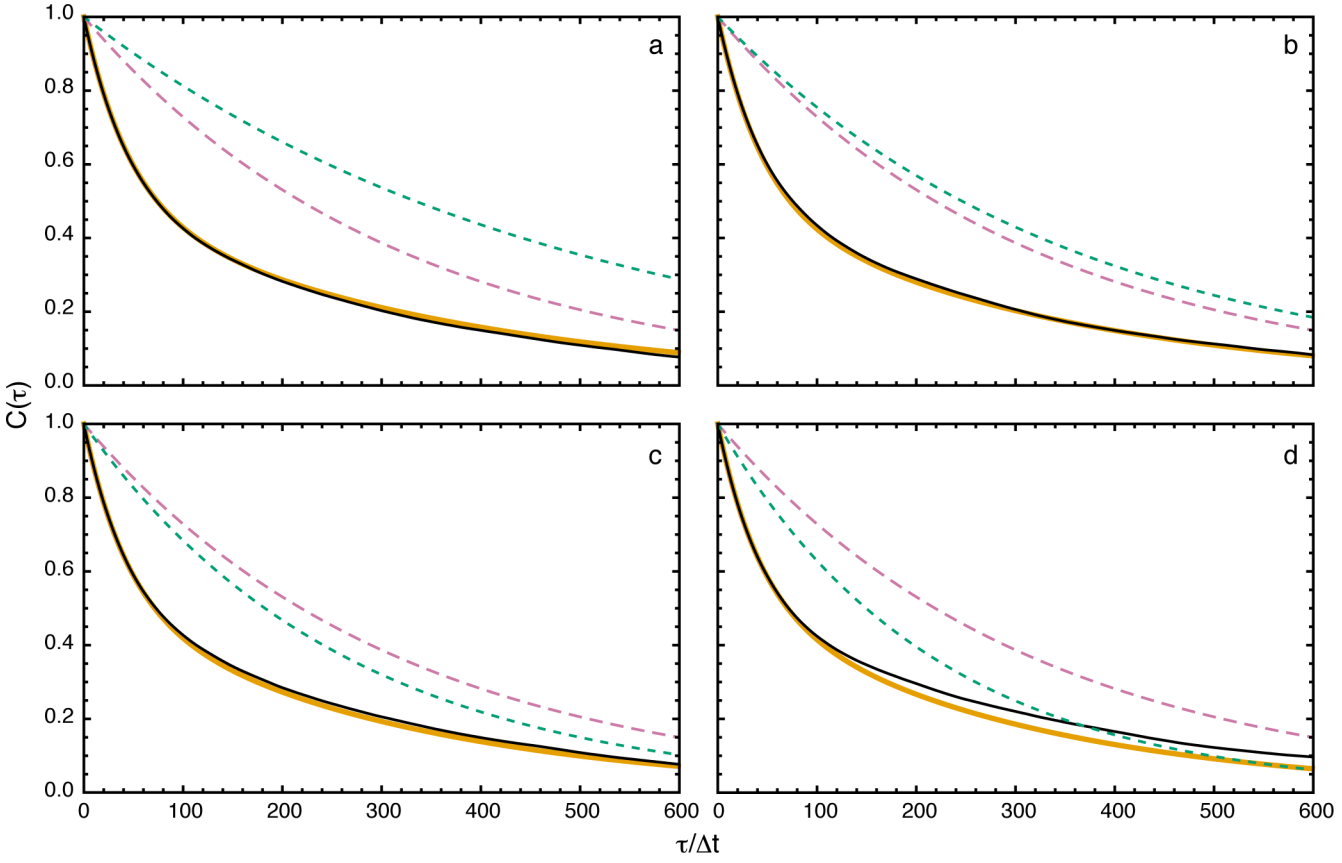

Figure 2. Comparison with simulations for different diffusion tensors. The plots show the correlation functions $C(\tau)$ for (thin, black lines) the simulation and (thick, orange lines) calculations from eqs 19, 20, and 25, (long dashed, reddish-purple lines) for the A diffusion tensor alone, and (short dashed, bluish-green lines) for the B diffusion tensor alone. Diffusion tensor B was varied as (a) $D_{xx}\Delta t = 2 \times 10^{-4}$, $D_{yy}\Delta t = 4 \times 10^{-4}$, and $D_{zz}\Delta t = 1.3 \times 10^{-3}$, (b) $D_{xx}\Delta t = 6 \times 10^{-4}$, $D_{yy}\Delta t = 3 \times 10^{-4}$, and $D_{zz}\Delta t = 1 \times 10^{-3}$, (c) $D_{xx}\Delta t = D_{yy}\Delta t = D_{zz}\Delta t = 6.3 \times 10^{-4}$, and (d) $D_{xx}\Delta t = 1 \times 10^{-3}$, $D_{yy}\Delta t = 6 \times 10^{-4}$, and $D_{zz}\Delta t = 3 \times 10^{-4}$. The values of $k_1\Delta t = 0.5 \times 10^{-2}$ and $k_2\Delta t = 1.5 \times 10^{-2}$. Other parameters are given in Methods.

dx.doi.org/10.1021/jp506580c | J. Phys. Chem. B 2014, 118, 11120–11128

in which $\tilde{\tau}_{mj} = 1/(6\tilde{D}_j)$ and local fast motions have been assumed to be similar in the different conformations. When $\tilde{\tau}_{mj}^2\omega_X^2 \gg 1$,

$$(R_2 - 0.5R_1)/R_1 \approx \frac{2}{3}\omega_X^2\langle\tilde{\tau}_{mj}\rangle\left\langle\frac{1}{\tilde{\tau}_{mj}}\right\rangle^{-1} \quad (28)$$

showing that relaxation rate constants depend upon the mean diffusion time and mean diffusion rate.

METHODS

Parameters for $N = 2$ site exchange between molecular conformations with distinct diffusion tensors are depicted in Figure 1. Orientational correlation functions $C(\tau) = P_2[\boldsymbol{\mu}(\tau)\cdot\boldsymbol{\mu}(0)]$, in which $\boldsymbol{\mu}(\tau)$ is a unit vector along the symmetry axis of the stochastic Hamiltonian, such as the N−H amide bond in a protein, were calculated by Monte Carlo simulations. Final correlation functions are the average of 25 individual simulations of 50,000 time steps. At each time step in a single simulation, the molecule is rotated around the *x*-, *y*-, and *z*-axes by angles chosen randomly from a Gaussian distribution with standard deviation $(2D_{\eta\eta})^{1/2}$ for the current conformation, in which $\eta = \{x, y, z\}$. After each diffusive step, the conformation of the molecule is switched between states if a random number drawn between 0 and 1 is greater than $p_j + p_{j'}\exp[-(k_1 + k_2)\,\Delta t]$, in which the molecule currently has the *j*th conformation. This protocol accurately reproduces the correlation functions for the individual diffusion tensors in the absence of kinetic exchange between conformations, and for the jump process in the absence of rotational diffusion (not shown). Model correlation functions were calculated using eqs 19, 20, and 25.

Initial simulations and calculations were performed with the following parameters. The spherical coordinates of the interaction unit vector in the A and B diffusion tensor frames were (72°, 37°) and (24°, 17°), respectively, and the Euler angles relating the two diffusion tensor frames were (27°, 78°, 17°), using the *zyz* convention. These values were chosen to be identical to those values used by Ryabov and co-workers in their Figure S1.[19] The diffusion tensor for state A was fixed with principal values $D_{xx}\Delta t = 3 \times 10^{-4}$, $D_{yy}\Delta t = 6 \times 10^{-4}$, and $D_{zz}\Delta t = 1 \times 10^{-3}$, in which Δt is the (arbitrary) time step for the simulations. Simulations were performed either by varying the diffusion tensor for the B state, while fixing the rate constants k_1 and k_2, or by fixing the diffusion tensor for the B state and varying k_1 and k_2. The average $(D_{xx} + D_{yy} + D_{zz})/3 = 6.33 \times 10^{-4}$ was equal for the A and B tensors in all cases. Additional details are given in the figure captions.

The structures of enzyme I in open and closed conformations were derived from PDB files 2L5H and 2HWG, respectively. The rotational diffusion tensors were calculated using HydroPro[26] with subsequent calculations performed using python.[27−29] The principal values of the diffusion tensor were calculated as $D_{xx} = 1.16 \times 10^6$ s^{-1}, $D_{yy} = 1.17 \times 10^6$ s^{-1}, and $D_{zz} = 2.50 \times 10^6$ s^{-1} for the open conformation. The principal axes are oriented with Euler angles (353.9°, 135.7°, 264.6°), relative to the frame of 2L5H. The closed conformation has a nearly isotropic diffusion tensor and for simplicity was treated as an isotropic sphere with an average diffusion constant of 2.46×10^6 s^{-1}. The two conformations were oriented by superposing the core domains, residues 270−573. After superposition of the core domains, the two diffusion frames were assumed to have the same orientation. Calculations assumed relative populations of 0.95 and 0.05 for open and closed conformations, respectively. Correlation functions were simulated for the N−H bond vectors of residues Leu 123, Val 246, and Arg 460. The spherical coordinates (θ, ϕ) of the interaction unit vector in the A (2L5H chain A, open) and B (2HWG chain A, closed) diffusion tensor frames were, respectively, (a) (42.8°, 80.7°) and (−62.6°, 38.6°), (b) (153.8°, 151.6°) and (142.9°, 85.0°), and (c) (116.4°, 74.7°) and (117.1°, 74.1°). The rate constant for transitions from closed to open conformations was $k_2 = 10^8$ s^{-1}. Relaxation rate constants R_1 and R_2 for the ^{15}N backbone amide spins were calculated for chain A of the enzyme I dimer using standard equations[21] and an N−H bond length of 1.02 Å, a chemical shift anisotropy of −170 ppm, and spectral density functions obtained from the Fourier transform of eq 19.

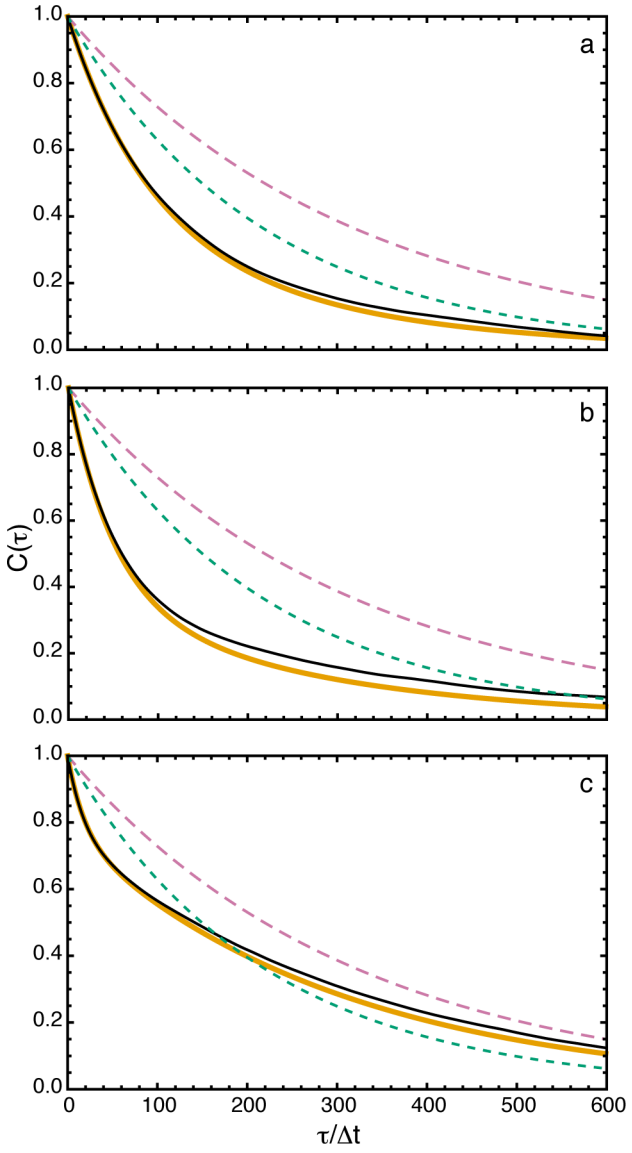

Figure 3. Comparison with simulations for different jump rates. The plots show the correlation functions $C(\tau)$ for (thin, black lines) the simulation and (thick, orange lines) calculations from eqs 19, 20, and 25, (long dashed, reddish-purple lines) for the A diffusion tensor alone, and (short dashed, bluish-green lines) for the B diffusion tensor alone. The values of (a) $k_1\Delta t = 0.5 \times 10^{-2}$ and $k_2\Delta t = 0.25 \times 10^{-2}$, (b) $k_1\Delta t = 0.7 \times 10^{-2}$ and $k_2\Delta t = 0.9 \times 10^{-2}$, and (c) $k_1\Delta t = 0.5 \times 10^{-2}$ and $k_2\Delta t = 4.5 \times 10^{-2}$. Figure 2d shows plots in the same series with $k_1\Delta t = 0.5 \times 10^{-2}$ and $k_2\Delta t = 1.5 \times 10^{-2}$. The diffusion tensor for the B state was fixed with principal values $D_{xx}\Delta t = 1 \times 10^{-3}$, $D_{yy}\Delta t = 6 \times 10^{-4}$, and $D_{zz}\Delta t = 3 \times 10^{-4}$. Other parameters are given in Methods.

dx.doi.org/10.1021/jp506580c | J. Phys. Chem. B 2014, 118, 11120−11128

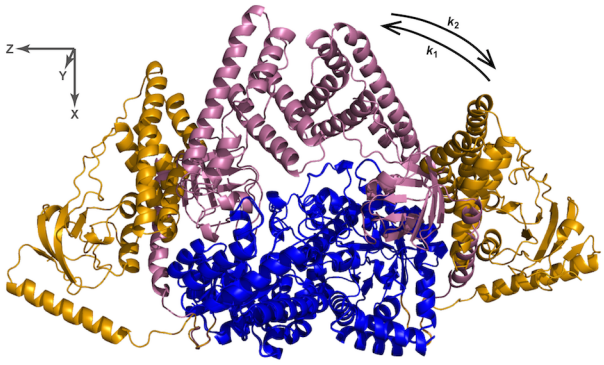

Figure 4. Structures of enzyme I in open and closed conformations derived from PDB files 2L5H and 2HWG, respectively. The two conformations were oriented by superposing the core inner domains, residues 270−573 (blue). The variable outer domains, residues 1−269, are orange (2L5H) and reddish-purple (2HWG).

The diffusion tensor for the rigid dumbbell structure of calmodulin, calculated from PDB file 1CLL, has principal values D_{xx} = 9.77 × 10^6 s^{-1}, D_{yy} = 10.2 × 10^6 s^{-1}, and D_{zz} = 20.4 × 10^6 s^{-1}. The principal axes are oriented with Euler angles (123.0°, 65.0°, 202.8°) relative to the frame of 1CLL. The diffusion tensor for the isolated N-terminal domain, residues 4−73, has D_{xx} = 32.9 × 10^6 s^{-1}, D_{yy} = 34.6 × 10^6 s^{-1}, and D_{zz} = 52.4 × 10^6 s^{-1}. The principal axes are oriented with Euler angles 93.3°, 88.5°, and 203.8° relative to the frame of 1CLL. The diffusion tensor for the C-terminal domain, residues 83−148, is nearly isotropic and for simplicity, the three principal values of the diffusion tensor were averaged to yield 42.1 × 10^6 s^{-1}. All diffusion tensors, relaxation rate constants, and spectral density functions were calculated as for enzyme I. Experimental data were fit to a model in the fast averaging limit between the rigid conformation and a conformation in which the central helix is disordered (consistent with the loss of data for residues in the central helix) and the N- and C-terminal domains reorient independently. The fitted model was optimized by minimizing the sum of the squared residuals between experimental and fitted R_2/R_1 ratios.

RESULTS AND DISCUSSION

To establish the accuracy of the suggested simplification to the general two-state diffusion problem, correlation functions calculated using eqs 19, 20, and 25 are compared to correlation functions obtained by Monte Carlo simulations. Figure 2 illustrates the effect of variations in the values of the diffusion tensor for the B state, while holding the A state diffusion tensor constant. The agreement between the simulated correlation functions and those obtained from the approximation of eq 25 is very good until the axial ratio of the B diffusion tensor becomes large (e.g., $2D_{zz}/(D_{xx} + D_{yy}) > 2$). Figures 2d and 3 show the effect of increasing rates of interconversion between conformations A and B, which also alters the equilibrium populations of the two states, while keeping the diffusion tensors constant. Again, the agreement between simulated and modeled correlation functions is excellent.

As a more realistic example, correlation functions and R_2/R_1 ratios were calculated for the symmetric 128 kDa dimeric complex of enzyme I, the first component of the phosphotransferase system of *Escherichia coli* (*E. coli*);[30] this model system was adopted by Ryabov and co-workers in their earlier work.[19] The protein is assumed to exchange between more

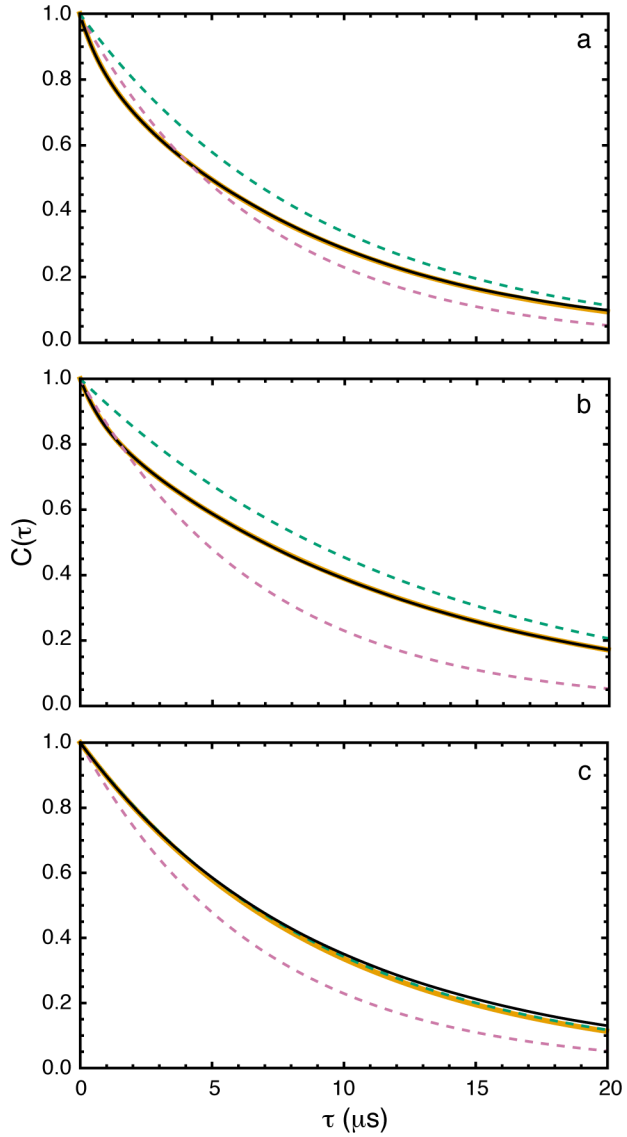

Figure 5. Sample correlation functions for (a) Leu 123, (b) Val 246, and (c) Arg 490 of enzyme I. Parameters for the calculations are given in Methods. The plots show the correlation functions $C(\tau)$ for (thin, black lines) the simulation and (thick, orange lines) calculations from eqs 19, 20, and 25, (long dashed, reddish-purple lines) for the open diffusion tensor alone and (short dashed, bluish-green lines) the closed diffusion tensor alone.

open and more closed conformations, corresponding to structures with PDB identification codes 2L5H and 2HWG, respectively, as depicted in Figure 4. In Figure 5, calculated correlation functions are shown for Leu 123 and Val 246, located in the outer domain, and Arg 490, located in the inner domain. Again, the agreement between the simulated correlation functions and the model functions calculated using eqs 19, 20, and 25 is excellent. Figure 6 shows calculated R_2/R_1 ratios for residues in enzyme I as functions of the interconversion rate constant for a fixed population of the open state of 0.95. For an axially symmetric molecule with a single conformation, which is well-approximated by the principal values of the diffusion tensor for the open state of enzyme I, the R_2/R_1 ratio is a function of $Y_{20}(\theta) = (3\cos^2\theta - 1)/2$, in which θ is the polar angle of the N−H bond vector in the principal axis coordinate system of the diffusion tensor.[23] Clearly, this ratio is

dx.doi.org/10.1021/jp506580c | J. Phys. Chem. B 2014, 118, 11120−11128

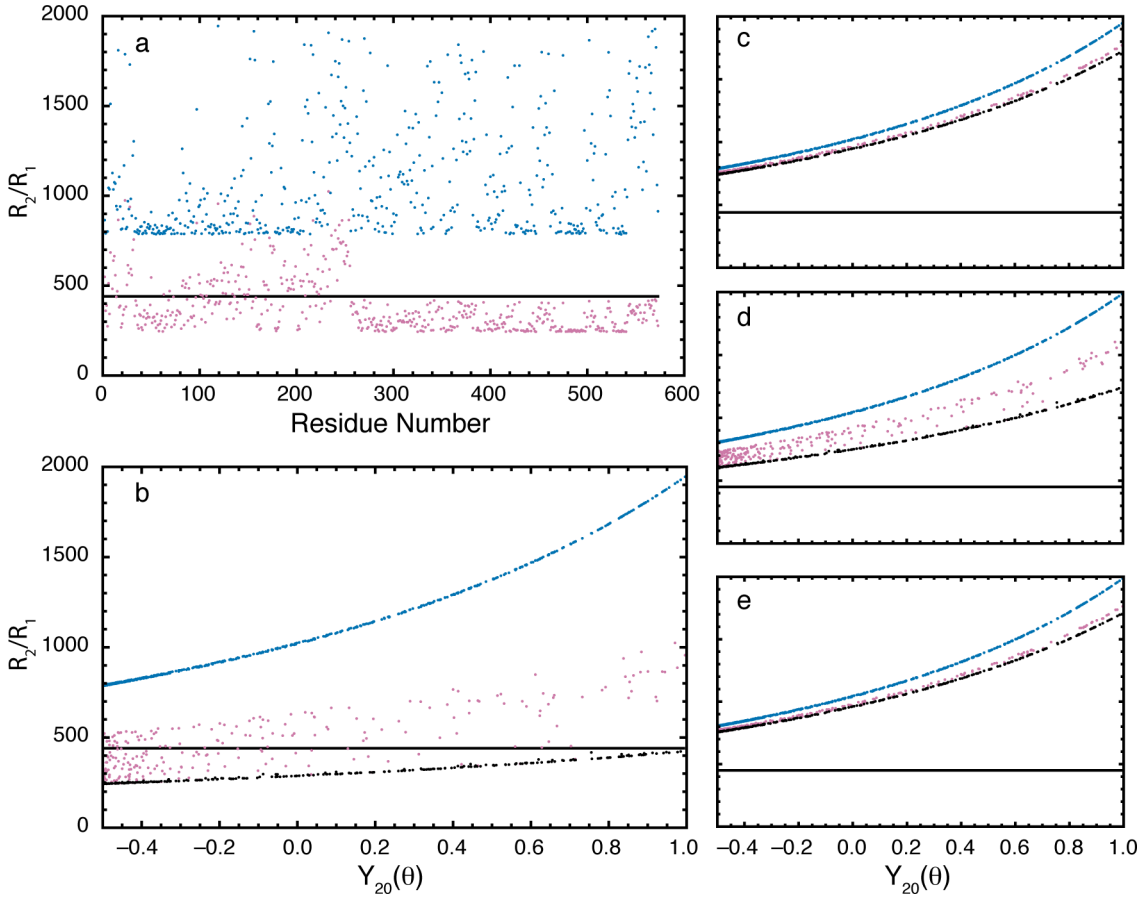

Figure 6. Calculated relaxation rate constants for enzyme I. The R_2/R_1 ratio is shown as a function of k_2, the rate constant for transitions from closed to open conformations. (a, b) The R_2/R_1 ratio is shown versus (a) the residue sequence position or (b) $Y_{20}(\theta) = (3\cos^2\theta - 1)/2$, in which θ is the polar angle of the N–H bond vector in the principal axis coordinate system of the open conformation for $k_2 = 10^8$ s^{-1}. Results are also shown as in panel b for (c) $k_2 = 10^6$ s^{-1}, (d) $k_2 = 10^{10}$ s^{-1}, and (e) $k_2 = 10^{11}$ s^{-1}. Other parameters are the same as those for Figure 5 and are given in Methods. In all panels, the horizontal black line and the blue symbols are the calculated results for the closed and open conformations, respectively. In panel a the reddish-purple symbols are the calculated results for the exchanging system. In the other panels, reddish-purple symbols are for residues in the outer domain (residues 1–269) and black symbols are for residues in the core inner domain (residues 270–573).

independent of $Y_{20}(\theta)$ for an isotropic molecule, which is well-approximated by the closed conformation of enzyme I. Parts a and b of Figure 6 show that the R_2/R_1 ratios differ strongly from the expected results from either the open or closed conformation alone. Residues in the inner core domain of enzyme I, residues 270–573, have nearly the same orientations in both conformations and primarily sense the different diffusional properties of the two states. In contrast, many residues in the outer domain, residues 1–269, have very different orientations in the two conformations and the R_2/R_1 ratios are very strongly perturbed by both the change in orientation and change in diffusion tensor between conformations. Parts b–e of Figure 6 show the effect of the kinetic rate constants from the slow (Figure 6c) to fast (Figure 6e) regimes. Figure 6c shows the averaging of the correlation functions for the two states in the slow limit, and Figure 6e shows the averaging of the diffusion tensors in the fast limit. In these two limits, the dependence of the R_2/R_1 ratios on $Y_{20}(\theta)$ is similar for residues in both the inner and outer domains. However, as shown in Figure 6b,d, when exchange is neither fast nor slow, the R_2/R_1 ratios for residues in the inner core and outer domains display very different dependencies on $Y_{20}(\theta)$. Thus, in this regime, interconversion between conformational states with different diffusion tensors can be recognized by departures of the R_2/R_1 ratios from the expected functional dependence on $Y_{20}(\theta)$. Notably, in this hypothetical case, a population of 0.05 for the minor closed state can be detected provided that good estimates of the diffusion tensors for the two exchanging conformations are available.

In practice, even a model with only two exchanging conformations has a large number of parameters, including the diffusion tensor principal values and axes systems, the relative orientation of the two diffusion frames, and the exchange kinetic rate constants. Fitting of experimental data is likely to be difficult without independent information about certain of the model parameters. As an illustration, Figure 7 shows experimental data reported by Chang and co-workers for[17] for calmodulin at 316 K. These data have been fit to a model in which the N- and C-terminal domains of calmodulin diffuse independently in state A (consistent with the loss of data for residues in the central helix) and the molecule has a rigid conformation with a stable central helix in state B. The experimental data are fit in the fast-exchange limit with a population of the B state of 0.68, yielding an average τ_m = 5.29 ns and S^2 = 0.13. The assumption that the A state can be modeled as independently tumbling N- and C-terminal domains is a simple approximation, which is unlikely to be strictly true because the domains are linked through the (disordered) central helix.

dx.doi.org/10.1021/jp506580c | J. Phys. Chem. B 2014, 118, 11120–11128

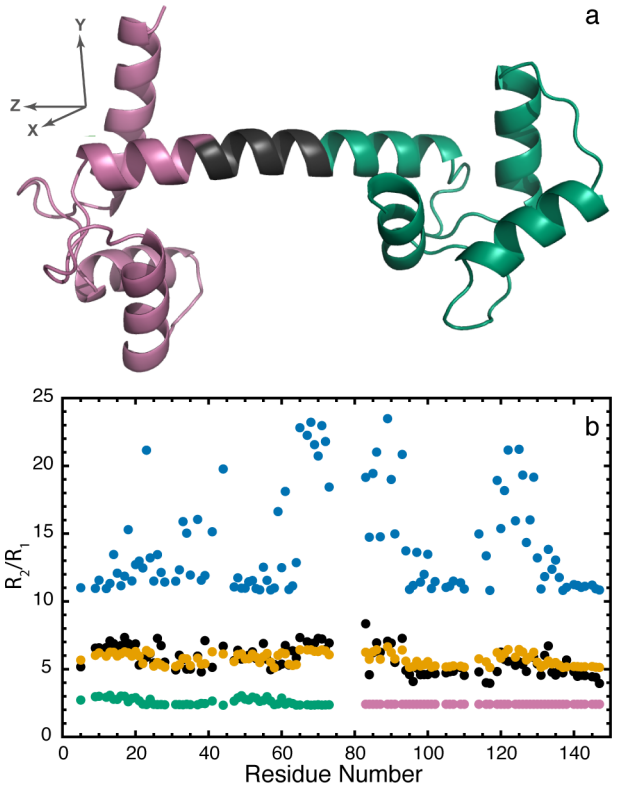

Figure 7. Fitted ^{15}N spin relaxation data for calmodulin acquired at 800 MHz and 316 K. (a) Structure of the rigid dumbbell structure from PDB file 1CLL. The N-terminal domain (residues 4−73) is bluish-green, and the C-terminal domain (residues 83−148) is reddish-purple. (b) (black) Experimental data reported by Chang and co-workers;[17] (blue) R_2/R_1 ratios calculated for the rigid dumbbell structure; (bluish-green) R_2/R_1 ratios calculated for the N-terminal domain; (reddish-purple) R_2/R_1 ratios calculated for the C-terminal domain; (orange) fitted model in the fast averaging limit between the rigid conformation and a conformation in which the central helix is disordered (consistent with the loss of data for residues in the central helix) and the N- and C-terminal domains reorient independently. The fitted model yields a population of the rigid dumbbell conformation of 0.68 in the fast-exchange limit. Other parameters for the calculations are given in Methods.

Consequently, this analysis is not intended to supplant the analysis of Chang and co-workers (which was based on more complete analysis of spin relaxation data acquired at three magnetic fields) or extensive investigations of calmodulin using residual dipolar couplings[31−33] and paramagnetic relaxation enhancements,[34−36] but only is intended to describe an approach to analyzing experimental data. These results also serve to indicate that different physical models can be fit to the same spin relaxation data in the absence of prior knowledge differentiating between alternatives. As noted, such additional data may be available from analysis of residual dipolar coupling constants[37,38] and paramagnetic relaxation enhancements.[39,40]

CONCLUSION

Ryabov and co-workers have derived an elegant solution for the orientational correlation function for molecules interconverting between states with different diffusion tensors.[19] This theory is very general and applies to proteins with arbitrary diffusion tensors for the different exchanging states. The present work shows that simpler results can be obtained for cases in which the diffusion tensors are only moderately asymmetric by combining the results of Wong and co-workers for isotropic systems[18] with the locally isotropic quadric diffusion approximation of Brüschweiler and co-workers.[20] The results of this work will be applicable to many systems of experimental interest, in which the diffusion tensors are not highly anisotropic, such as calmodulin and enzyme I, or for exploring the relationship between various parameters in an exchange model prior to rigorous numerical optimization with the complete formalism of Ryabov and co-workers.

AUTHOR INFORMATION

Corresponding Author

*E-mail: agp6@columbia.edu. Tel.: (212) 305-8675. Fax: (212) 305-7932.

Notes

The authors declare no competing financial interest.

ACKNOWLEDGMENTS

This work was supported by National Institutes of Health Grants GM059273 (A.G.P.) and GM089047 (M.L.G.). Alek Eren is thanked for programming assistance at an early stage of this work. Helpful discussions with Mark Rance are acknowledged gratefully.

REFERENCES

(1) Kowalewski, J.; Mäler, L. *Nuclear Spin Relaxation in Liquids: Theory, Experiments, and Applications*; Taylor and Francis: New York, 2006.

(2) Palmer, A. G. NMR Characterization of the Dynamics of Biomacromolecules. *Chem. Rev.* **2004**, *104*, 3623−3640.

(3) Palmer, A. G. In *Biophysical Techniques for Structural Characterization of Macromolecules*; Dyson, H. J., Ed.; Academic Press: Oxford, U.K., 2012; pp 216−244.

(4) Jarymowycz, V. A.; Stone, M. J. Fast Time Scale Dynamics of Protein Backbones: NMR Relaxation Methods, Applications, and Functional Consequences. *Chem. Rev.* **2006**, *106*, 1624−1671.

(5) Lipari, G.; Szabo, A. Model-Free Approach to the Interpretation of Nuclear Magnetic Resonance Relaxation in Macromolecules. 1. Theory and Range of Validity. *J. Am. Chem. Soc.* **1982**, *104*, 4546−4559.

(6) Lipari, G.; Szabo, A. Model-Free Approach to the Interpretation of Nuclear Magnetic Resonance Relaxation in Macromolecules. 2. Analysis of Experimental Results. *J. Am. Chem. Soc.* **1982**, *104*, 4559−4570.

(7) Halle, B.; Wennerström, H. Interpretation of Magnetic Resonance Data from Water Nuclei in Heterogeneous Systems. *J. Chem. Phys.* **1981**, *75*, 1928−1943.

(8) Schurr, J. M.; Babcock, H. P.; Fujimoto, B. S. A Test of the Model-Free Formulas. Effects of Anisotropic Rotational Diffusion and Dimerization. *J. Magn. Reson., Ser. B* **1994**, *105*, 211−224.

(9) Clore, G. M.; Szabo, A.; Bax, A.; Kay, L. E.; Driscoll, P. C.; Gronenborn, A. M. Deviations from the Simple Two-Parameter Model-Free Approach to the Interpretation of Nitrogen-15 Nuclear Magnetic Relaxation of Proteins. *J. Am. Chem. Soc.* **1990**, *112*, 4989−4991.

(10) Shapiro, Y. E. NMR Spectroscopy on Domain Dynamics in Biomacromolecules. *Prog. Biophys. Mol. Biol.* **2013**, *112*, 58−117.

(11) Meirovitch, E. SRLS Analysis of ^{15}N Relaxation from Bacteriophage T4 Lysozyme: A Tensorial Perspective That Features Domain Motion. *J. Phys. Chem. B* **2012**, *116*, 6118−6127.

(12) Meirovitch, E.; Shapiro, Y. E.; Polimeno, A.; Freed, J. H. Structural Dynamics of Bio-Macromolecules by NMR: The Slowly Relaxing Local Structure Approach. *Prog. Nucl. Magn. Reson. Spectrosc.* **2010**, *56*, 360−405.

(13) Emani, P. S.; Olsen, G. L.; Varani, G.; Drobny, G. P. Theory of Nonrigid Rotational Motion Applied to NMR Relaxation in Rna. *J. Phys. Chem. A* **2011**, *115*, 12055−12069.
(14) Kotsyubynskyy, D.; Zerbetto, M.; Soltesova, M.; Engstrom, O.; Pendrill, R.; Kowalewski, J.; Widmalm, G.; Polimeno, A. Stochastic Modeling of Flexible Biomolecules Applied to NMR Relaxation. 2. Interpretation of Complex Dynamics in Linear Oligosaccharides. *J. Phys. Chem. B* **2012**, *116*, 14541−14555.
(15) Baber, J. L.; Szabo, A.; Tjandra, N. Analysis of Slow Interdomain Motion of Macromolecules Using NMR Relaxation Data. *J. Am. Chem. Soc.* **2001**, *123*, 3953−3959.
(16) Chang, S.-L.; Tjandra, N. Analysis of NMR Relaxation Data of Biomolecules with Slow Domain Motions Using Wobble-in-a-Cone Approximation. *J. Am. Chem. Soc.* **2001**, *123*, 11484−11485.
(17) Chang, S.-L.; Szabo, A.; Tjandra, N. Temperature Dependence of Domain Motions of Calmodulin Probed by NMR Relaxation at Multiple Fields. *J. Am. Chem. Soc.* **2003**, *125*, 11379−11384.
(18) Wong, V.; Case, D. A.; Szabo, A. Influence of the Coupling of Interdomain and Overall Motions on NMR Relaxation. *Proc. Natl. Acad. Sci. U. S. A.* **2009**, *106*, 11016−11021.
(19) Ryabov, Y.; Clore, G. M.; Schwieters, C. D. Coupling between Internal Dynamics and Rotational Diffusion in the Presence of Exchange between Discrete Molecular Conformations. *J. Chem. Phys.* **2012**, *136*, No. 034108.
(20) Brüschweiler, R.; Liao, X.; Wright, P. E. Long-Range Motional Restrictions in a Multidomain Zinc-Finger Protein from Anisotropic Tumbling. *Science* **1995**, *268*, 886−889.
(21) Cavanagh, J.; Fairbrother, W. J.; Palmer, A. G.; Rance, M.; Skelton, N. J. *Protein NMR Spectroscopy: Principles and Practice*, 2nd ed.; Academic Press: San Diego, CA, USA, 2007.
(22) Abergel, D.; Palmer, A. G. On the Use of the Stochastic Liouville Equation in NMR: Application to $R_{1\rho}$ Relaxation in the Presence of Exchange. *Concepts Magn. Reson.* **2003**, *19A*, 134−148.
(23) Lee, L. K.; Rance, M.; Chazin, W. J.; Palmer, A. G. Rotational Diffusion Anisotropy of Proteins from Simultaneous Analysis of ^{15}N and $^{13}C^{\alpha}$ Nuclear Spin Relaxation. *J. Biomol. NMR* **1997**, *9*, 287−298.
(24) Ban, D.; Sabo, T. M.; Griesinger, C.; Lee, D. Measuring Dynamic and Kinetic Information in the Previously Inaccessible Supra-T_c Window of Nanoseconds to Microseconds by Solution NMR Spectroscopy. *Molecules* **2013**, *18*, 11904−11937.
(25) Lange, O. F.; Lakomek, N.-A.; Fares, C.; Schroeder, G. F.; Walter, K. F. A.; Becker, S.; Meiler, J.; Grubmueller, H.; Griesinger, C.; de Groot, B. L. Recognition Dynamics Up to Microseconds Revealed from an RDC-Derived Ubiquitin Ensemble in Solution. *Science* **2008**, *320*, 1471−1475.
(26) Ortega, A.; Amoros, D.; Garcia de la Torre, J. Prediction of Hydrodynamic and Other Solution Properties of Rigid Proteins from Atomic- and Residue-Level Models. *Biophys. J.* **2011**, *101*, 892−898.
(27) van der Walt, S.; Colbert, S. C.; Varoquaux, G. The Numpy Array: A Structure for Efficient Numerical Computation. *Comput. Sci. Eng.* **2011**, *13*, 22−30.
(28) Pérez, F.; Granger, B. E. IPython: A System for Interactive Scientific Computing. *Comput. Sci. Eng.* **2007**, *9*, 21−29.
(29) McKinney, W. Data Structures for Statistical Computing in Python. *Proceedings of the 9th Python in Science Conference*, **2010**, 51−56.
(30) Schwieters, C. D.; Suh, J. Y.; Grishaev, A.; Ghirlando, R.; Takayama, Y.; Clore, G. M. Solution Structure of the 128 kDa Enzyme I Dimer from *Escherichia coli* and Its 146 kDa Complex with HPr Using Residual Dipolar Couplings and Small- and Wide-Angle X-ray Scattering. *J. Am. Chem. Soc.* **2010**, *132*, 13026−13045.
(31) Biekofsky, R. R.; Muskett, F. W.; Schmidt, J. M.; Martin, S. R.; Browne, J.; Bayley, P. M.; Feeney, J. NMR Approaches for Monitoring Domain Orientations in Calcium-Binding Proteins in Solution Using Partial Replacement of Ca^{2+} by Tb^{3+}. *FEBS Lett.* **1999**, *460*, 519−526.
(32) Chou, J. J.; Li, S.; Klee, C. B.; Bax, A. Solution Structure of Ca^{2+}—Calmodulin Reveals Flexible Hand-Like Properties of Its Domains. *Nat. Struct. Biol.* **2001**, *8*, 990−997.
(33) Bertini, I.; Del Bianco, C.; Gelis, I.; Katsaros, N.; Luchinat, C.; Parigi, G.; Peana, M.; Provenzani, A.; Zoroddu, M. A. Experimentally Exploring the Conformational Space Sampled by Domain Reorientation in Calmodulin. *Proc. Natl. Acad. Sci. U. S. A.* **2004**, *101*, 6841−6846.
(34) Anthis, N. J.; Doucleff, M.; Clore, G. M. Transient, Sparsely Populated Compact States of Apo and Calcium-Loaded Calmodulin Probed by Paramagnetic Relaxation Enhancement: Interplay of Conformational Selection and Induced Fit. *J. Am. Chem. Soc.* **2011**, *133*, 18966−18974.
(35) Russo, L.; Maestre-Martinez, M.; Wolff, S.; Becker, S.; Griesinger, C. Interdomain Dynamics Explored by Paramagnetic NMR. *J. Am. Chem. Soc.* **2013**, *135*, 17111−17120.
(36) Bertini, I.; Luchinat, C.; Nagulapalli, M.; Parigi, G.; Ravera, E. Paramagnetic Relaxation Enhancement for the Characterization of the Conformational Heterogeneity in Two-Domain Proteins. *Phys. Chem. Chem. Phys.* **2012**, *14*, 9149−9156.
(37) Maciejewski, M.; Tjandra, N.; Barlow, P. N. Estimation of Interdomain Flexibility of N-Terminus of Factor H Using Residual Dipolar Couplings. *Biochemistry* **2011**, *50*, 8138−8149.
(38) Bertini, I.; Giachetti, A.; Luchinat, C.; Parigi, G.; Petoukhov, M. V.; Pierattelli, R.; Ravera, E.; Svergun, D. I. Conformational Space of Flexible Biological Macromolecules from Average Data. *J. Am. Chem. Soc.* **2010**, *132*, 13553−13558.
(39) Clore, G. M. Seeing the Invisible by Paramagnetic and Diamagnetic NMR. *Biochem. Soc. Trans.* **2013**, *41*, 1343−1354.
(40) Clore, G. M. Interplay between Conformational Selection and Induced Fit in Multidomain Protein-Ligand Binding Probed by Paramagnetic Relaxation Enhancement. *Biophys. Chem.* **2014**, *186*, 3−12.